ISSN: 1992-8645 www.jatit.org E-ISSN: 1817-3195

PIXEL-BASED ALGORITHM IN BRAIN TUMOR CLASSIFICATION MEASURING AREA

DWI SWASONO RACHMAD[1*], JOHAN HARLAN[2], MOHAMMAD IQBAL

[1]Department Computer Science, Bhayangkara University, Jakarta, Indonesia
[23]Department Information Technology, Gunadarma University, Depok, Indonesia

**Email : [1]dwi.swasono@dsn.ubharajaya.ac.id, [2]harlan_johan@staffsite.gunadarma.ac.id, mohiqbal@staff.gunadarma.ac.id*

ID 55522 Submission	Editorial Screening	Conditional Acceptance	Final Revision Acceptance
08-09-2024	08-09-2024	25-09-2024	08-10-2024

ABSTRACT

Magnetic Resonance Imaging (MRI) is a medical computer technology that can be utilized for the diagnosis of brain cancers. MRI is a medical imaging technique that utilizes magnetic fields based on the principles of computed tomography. Nevertheless, there are still deficiencies in the areas of interpretation, temporal analysis, and visualization. The primary objective of this study is to identify the precise features of the Glioma tissue, including its location and size. The study utilized MRI images in bmp format obtained from the Cipto Mangunkusumo Jakarta Central General Hospital. The study focused on developing algorithms using active contour methods, otsu method, and hybrid method. Additionally, the study incorporated object detection ROI combined with region feature methods. The area of the glioma was calculated using Matlab and Python tools throughout the testing phase. This study utilizes imaging data from 13 T1 contrasted axial sequence components.

The outcome of the segmentation and extraction method is utilized to compute the glioma's area, which is determined by the pixels that have undergone processing. The hybrid method effectively distinguishes the object under study from other objects. This method achieves an average accuracy rate of 99% when using numerical methods that involve absolute and relative error calculations, as well as extraction segmentation processes with template matching algorithms. The average precision value of +1 indicates that feature extraction with a hybrid approach is dependable for clinical evaluation

Keywords: *Brain Tumor, Hybrid, MRI, Pixel, Template Matching*

1. INTRODUCTION

The domain of computer science and communication is intricately linked to human labor [1]. Thanks to technological advancements in the sphere of communication media, which are based on the foundations of information technology [2]. Computer media has exhibited a diverse range of sizes, spanning from compact devices to expansive systems, all showcasing remarkable performance capabilities [3] [4] [5]. In addition, technology has greatly enhanced different areas of human labor by enabling faster, more efficient, and more economical operational operations [6].

Health professionals continue to use manual techniques, the MRI provider's application viewer, and mathematical morphology embedded in computer science calculations for measuring the remaining portion of the tumor object that requires manual measurement, particularly the diatarsis. Nevertheless, because the tumor in this instance has a range of forms, kinds, depths, and incisions, the image acquired during the detection process using an MRI machine is still far from accurate in identifying the location of the tumor item. In computer science, manual research methods are no longer viable, so researchers need to be able to perform a variety of processing operations on images that are created using viewers. However, no pixel approach has been used yet, which would allow data to be processed without sacrificing the values or characteristics of MRI image datasets.

Further study aims to build on previously conducted studies in order to process and assess MRI image measurements using a pixel-by-pixel approach.

In order to streamline treatment interventions and clinical trials, it is necessary to conduct a concise and thorough assessment of GBM [7]. Considering the circumstances, it appears that creating a volume strategy would be a more prudent decision. The rationale for the importance of the advancement, regularity, and availability of the segmentation strategy is vital. This study demonstrates a robust correlation between the ellipsoid formula and hand segmentation in accurately predicting the volume of the GBM division [8]. This association is mostly observed in the precise determination of the patient's reaction to treatment, as classified by the four RANO groups. According to the results, the use of an ellipsoid formula can be beneficial for measuring in clinical scenarios [9].

The morphology and dimensions of the hematoma, together with individual differences, can impact the utilization of the Tada method for quantifying intracerebral bleeding (ICH) [10]. The volume range of 20-40 ml exhibits reduced inter-observer reliability, leading to potential inaccuracies in disease assessment and therapy. Implementing ways to address the limitations mentioned above and enhance the accuracy of the quantity measured [11] is crucial in evaluating two distinct techniques for measuring the volume of intracerebral hemorrhage (ICH) [12]. The two methods used are software-aided planimetry and the elliptical volume approach, generally known as ABC/2. Section [13] [14]:

A multitude of methods for viewing tumor volumes are elucidated in a series of current scientific studies [15], commencing with the utilization of multiple two-dimensional photographs. Several studies indicate that the hemi-ellipsoids provide a realistic representation of the tumor's three-dimensional shape. To determine three crucial dimensions, namely height [16], breadth, and length, it is necessary to have estimates of tumor volume [17].

A new system to categorize hemi-ellipsoid brain tumors is presented by the author. Using mathematical morphology, this approach utilizes active contour approaches, Otsu methods [18], basic morphological operations, and data extraction [19]. According to this research, the technique that previously used a mathematical approach is not good, but it needs a pixel approach in the field of computer science between algorithms as well as previous research, has not known the shortcomings for the algority used either or errors as comparisons between the algoritms and also with the matching between the tumor area objects of the algoritm being studied. The comparison with the size of the pixels [20] as a measure to distinguish between different types of cancer. Shapes performed with otsu algorithms, active contours [21] and using microdicom [22] application calculations will be used in the evaluation process as well as hybrid [23] algoritms like brain tumors, when classifying [24] items based on detection.

2. METHOD

This analysis utilized magnetic resonance imaging data (MRI) obtained from the data collection of the General Hospital of Cipto Mangunkusumo Center [25]. This dataset offers statistics regarding the incidence of cerebrovascular illness. The data [26] [27] comprises a collection of clinically obtained information regarding brain tumors from the RSUP Department of Radiology Cipto Mangun Kusumo. A qualified neuroradiologist [27] is required to regularly update the dataset and supply fundamental truth labels. After being acquired, magnetic resonance imaging (MRI) is then digitized and stored. Figure 1 displays the compilation of photographs from the investigation.

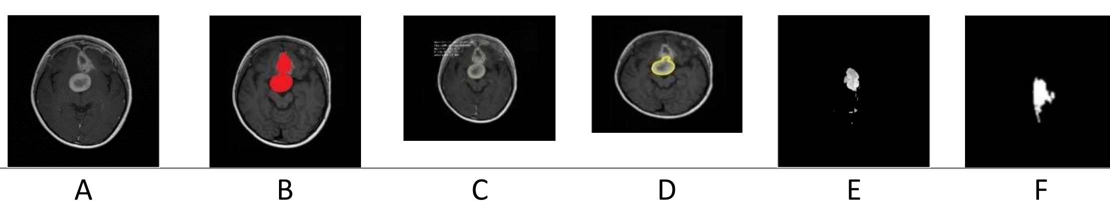

Figure 1 Original MRI picture (A), Ground Truth (B), Microdicom (C), Active Contour (D), Otsu (E), Hybrid(F)

The design given by this study consists of three primary phases: (1) Saving photographs in the BMP image format[28]. (2) Establishing ground truth[29] as the fundamental reference values for comparison with alternative [30] methods in the future; (3) Employing active, Otsu, and hybrid contour algorithms with extended morphological [31] processes for brain tumor segmentation, along with calculations using microdicom applications. Several algorithms are employed, which begin by establishing ground truth and involve extensive computation using tools such as microdecom viewer, otsu, active contours, and hybrids. These algorithms are typically utilized to extract statistical information from photographs. Furthermore, the extraction procedure considers the dimensions of the pixels associated with each approach.

2.1 Dataset

This approach necessitates the submission of precise and validated data regarding the precise location of the tumor illustrated in the image [32] [33]. This information will provide as training data and a standard for evaluating various research methodologies, such as manual mathematical morphology, pixel-based segmentation and extraction methods without manual intervention, and template matching algorithms. Subsequently, the image region is precisely defined in order to differentiate the intended primary topic from the encompassing background. In order to continue, it is necessary to utilize complex algorithms to guarantee accurate numerical values for every image [34].

2.2.2 Segmentation

The active contour methodology is employed for segmenting MRI images that have undergone prior processing. Figure 1 employs oxygen, active contour, and hybrid approaches for the purpose of detecting brain cancer. Magnetic resonance imaging (MRI) segmentation is employed to detect regions with distinct features that indicate the presence of brain tumors. It also helps differentiate between tumor and non-tumor entities by analyzing the RGB values retrieved from MRI images [35].

2.2.3 Extraction

Extraction is the primary phase to be carried out as a basis for finding complete information from the image to be researched.

a. Create Ground Truth
Calculations using ground truth data are utilized to obtain fundamental benchmark values derived from alternative techniques [36] [37]. The given MRI image (Figure 1B) will serve as a reference point for comparison with other algorithms. Ground truth will be established, and a certain tumor location has been designated as the baseline value [38].

b. Dataset derived from microdicom applications
The dataset is derived from the original MRI data obtained using the Microdicom MRI viewer tool. The MRI image displayed (Figure 1 C) above is generated by processing the data set using the microdicom application. The application provides features that facilitate the user in determining the size of the tumor area.

c. Datasets based on active contours
The segmentation method in this process employs an active contour, which is a closed curve that can dynamically expand or contract to accurately delineate the image. Here is the initial MRI image that will undergo processing. The active contour method has been employed to segment the MRI picture, wherein the contour adapts to the targeted brain tumor location within the image. Once the detection is complete, the object will be marked with a yellow indicator, signifying that the image has successfully identified and selected the object using the activated contour (Figure 1 D).

d. Datasets based on Otsu algorithms

The segmentation approach in this process employs the Otsu method. This approach calculates the distribution of picture intensity and image weight, and provides a threshold value of 256. When the image value is altered in advanced study, the image will be transformed into a white color. Here is the initial MRI image that has to be analyzed.

Figure 2 Results of Otsu's MRI algorithm

The extraction process involves utilizing the Otsu thresholding algorithm, followed by contour detection. This process entails identifying a bounding box around the tumor and marking it in blue to facilitate differentiation between images without tumors and those with tumors.

e. Hybrid Algorithm-Based Datasets

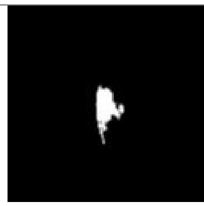

Figure 3 Hybrid algorithm MRI results

The hybrid technique involves multiple procedures, such as picture acquisition and the utilization of acoustic thresholding in conjunction with the active contour method. This procedure starts with the initial acquisition of the MRI image. Next, the Otsu thresholding technique is applied to assign a label to the object in the image. Finally, active contours are used to segment the image. The next approach involves employing the active contour method for detection. This method identifies photos with similarities and adapts to the indicated image object for detection

f. Pixel calculation

The procedure involves employing many techniques, including the employment of microdicom MRI viewer software, Otsu procedures, active contours, and hybrids. The subsequent actions are executed:

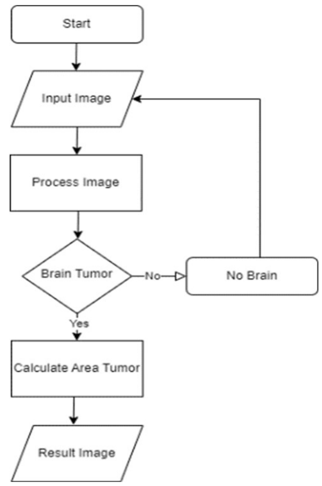

Figure 4 Measurement Method Circuit Diagram

The aforementioned procedures involve the primary procedure of segmenting and extracting using the microdicom, otsu, active contour, and hybrid methods with a pixel-based methodology approach

g. Template Matching Algorithm

At this stage, the method will utilize a pixel-based template matching algorithm acquired via segmentation processing. The extraction of pixels will be performed using a variety of methods, including approaches using the microdicom program, active contours, otsu, and hybrids. The selected approach will depend on the fundamental truth as the benchmark value. After implementing the approach, the advanced procedure will utilize the pixel template matching algorithm [39].

The survey undertaken by involves the comparison of each pixel in a digital picture matrix with a template image using this technique. Template matching using equations:

$$r = \frac{\sum_{k=1}^{N}(x_{ik}-\bar{x}).(y_{jk}-\bar{y})}{\sqrt{\sum_{k=1}^{N}(x_{ik}-\bar{x})^2.\sum_{k=1}^{N}(y_{jk}-\bar{y})^2}} \quad (1)$$

The correlation coefficient, denoted as r, is the measure of correlation between two variables. In this context, xik refers to the image that serves as the reference, while $\bar{x}$ represents the average value of the image.

h. Algorithm error

Accuracy is commonly defined as the degree to which a quantitative measurement deviates from the true value[40]. When performing computations using numerical methods, it is crucial to conduct error analysis. The error magnitude quantifies the precision of the numerical solution, reflecting its proximity to the correct answer

True value = Approximation + Error If the margin value against the true value is a, then the difference is called Error.

In the field of numerical techniques, failure, sometimes referred to as error, refers to the discrepancy between the actual value and the value produced by the iterative process aimed at approaching the true value. Nevertheless, employing an inaccurate numerical approach does not imply that the outcome is completely unreliable; it is possible to decrease mistakes to the greatest extent feasible, resulting in a result that is quite proximate to the actual number, or even approaching zero.

Within the field of numerical techniques, accuracy can be assessed by two distinct measures: absolute error and relative error. An absolute mistake is the absolute value of the difference between the real value x and the observed value x'

$$\epsilon_A = |x - x'| \qquad (2)$$

A relative error is calculated by dividing the difference between the actual value x and the observed value x' by the actual value, as opposed to an absolute error. The outcome obtained is a value without any associated unit. The equation for relative error is displayed below.

$$\epsilon_R = \left|\frac{x - x'}{x}\right| 100\% \qquad (3)$$

Precision is the frequency with which measurements are conducted under same conditions, yielding consistent outcomes. In this case for the calculation of absolute error and relative error on numerical methods as follows:

1. Error Absolutely

$$\epsilon_A = |357 - 1008|$$

2. Error Relative

$$\epsilon_R = \left|\frac{357 - 1008}{357}\right| 100\%$$

3. Percentage

Formula:

$$Accuracy = \frac{Ground\ Truth\ Value}{Value\ Obtained} 100\%$$

or

$$Accuracy = 100\% - Value\ Obtained$$

3. RESULT AND DISCUSSION

Software utilized for MRI imaging operations includes Matlab and Python. The utilization of Otsu algorithms, active and hybrid contours, along with the application of MicroDicom software, enables the measurement of tumor regions. The endeavor necessitates the use of segmented MRI scans to precisely isolate the particular region of the tumor within each object. Furthermore, the methodology employed microdicom applications, active contour, Otsu, and hybrid techniques to generate MRI pictures of the Axial T1 Contracts type, with dimensions of 256x256 pixels. In this situation, the algorithms have been used to acquire the result. The computation of the error can be followed using the algorithm that has been implemented as described below:

a. Results Algorithm Error

Table 1 Calculation of Absolute Error Based on Numerical Methods

Basic Value

ISSN: 1992-8645 www.jatit.org E-ISSN: 1817-3195

No	Ground Truth	Active Contour	Microdicom	Otsu	Hybrid
1	357	1008	691	209	340
		Error Absolut			
		Active Contour	Microdicom	Otsu	Hybrid
		-651	-334	148	17

The absolute error calculations in Table 1 are derived from numerical methods. The value is derived through the utilization of the ground truth formation process, the active contour methodology, the microdicom viewer, the otsu methodology, and culminates with the hybrid process. The base value is derived from processing various methods applied to glioma MRI image segmentation. Once obtained, the value is scaled to calculate the absolute error between the base value and the actual value. The table shows the minimum error value for the hybrid method, while the active contour method yields the maximum value. The hirbid method is a fusion of the otsu method and the active contour method.

Table 2 Relative Error Calculation Based on Numerical Methods

		Basic Value			
No	Ground Truth	Active Contour	Microdicom	Otsu	Hybrid
1	357	1008	691	209	340
		Error Absolut			
		Active Contour	Microdicom	Otsu	Hybrid
		-182%	-94%	41%	5%

Calculate the relative error using numerical methods in table 2. The value is derived by the utilization of the ground truth formation process, the active contour methodology, the microdicom viewer, the otsu methodology, and the hybrid process. Basic values are derived from the analysis of glioma MRI image slices using various methodologies. Once the values have been acquired, the error value is determined by scaling the difference between the base value and the relative error. The hybrid approach exhibits the minimum error value in the table, whereas the active contour method demonstrates the maximum value. The hirbid method is a fusion of the otsu method and the active contour method. The resulting hybrid value is the error percentage, which is 5%.

Table 3 Percentage Calculation Based on Numerical Methods

		Basic Value			
No	Ground Truth	Active Contour	Microdicom	Otsu	Hyrbid
1	357	1008	691	209	340
		Error Absolut			
		Active Contour	Microdicom	Otsu	Hybrid
		282%	194%	59%	95%

Calculate accuracy using numerical methods based on the data provided in table 3.3. The value is derived by the utilization of the ground truth formation process, the active contour methodology, the microdicom viewer, the otsu methodology, and the hybrid process. The base value is derived from the processing of several methods applied to an MRI image of a glioma, specifically acquired by chopping the image. Once the desired value is attained, it is determined by subtracting the error value from 100% accuracy, which is obtained through reduction cutting. The outcome is determined by the cutting value, which is set at 100% initially and then reduced to 95% in the hybrid approach. The highest value is obtained when employing the active contour computation.

b. *Results Algoritm Template Matching*

This algorithm utilizes various algorithms, such as Otsu, active, and hybrid contours, to compare and match the results of image processing. Additionally, it compares the calculated result obtained from a microdicom viewer application. The purpose of this algorithm is to identify images in the form of letters, numbers, bookmarks, and other applications that involve image matching. In order to determine whether a PCB image is free of flaws or not, a correlation value of 1 indicates that it is good, while a correspondence value of -1 indicates the presence of total defects. The formula employed is:

$$r = \frac{\sum_{k=1}^{N}(x_{ik} - \bar{x}).(y_{jk} - \bar{y})}{\sqrt{\sum_{k=1}^{N}(x_{ik} - \bar{x})^2.\sum_{k=1}^{N}(y_{jk} - \bar{y})^2}}$$

The equation provided indicates that "r" represents the correlation coefficient, "xik" represents the image that serves as the reference, and "x̄" represents the average value of the reference image. Let y represent the input image, represent the average of the input picture, and n represent the number of pixels in the image.

The equation provided allows for the implementation of a sophisticated hybrid approach that involves the pixel acquisition unit. This method can then be further enhanced through the utilization of the template matching algorithm, which operates according to the following specifications:

a) Comparing the outcomes of template matching with active contours

$$r = \frac{\sum_{k=1}^{13}(2090 - 1389).(2601 - 1683)}{\sqrt{\sum_{k=1}^{13}(2090 - 1389)^2.\sum_{k=1}^{13}(2601 - 1683)^2}} = -1$$

b) Results of template matching using microdicom

$$r = \frac{\sum_{k=1}^{13}(2090 - 1389).(8806 - 4908)}{\sqrt{\sum_{k=1}^{13}(2090 - 1389)^2.\sum_{k=1}^{13}(8806 - 4908)^2}} = -1$$

c) The results involve the matching of a template with the Otsu method.

$$r = \frac{\sum_{k=1}^{13}(2090 - 1389).(1748 - 1311)}{\sqrt{\sum_{k=1}^{13}(2090 - 1389)^2.\sum_{k=1}^{13}(1748 - 1311)^2}} = -1$$

d) Utilizing hybrid template matching for matching purposes.

$$r = \frac{\sum_{k=1}^{13}(2090 - 1389).(2084 - 1360)}{\sqrt{\sum_{k=1}^{13}(2090 - 1389)^2.\sum_{k=1}^{13}(2084 - 1360)^2}} = 1$$

The segmentation procedure and initial extraction are completed. The processing was conducted using a pixel-based methodology, beginning with the utilization of ground truth, otsu, active and hybrid contours for processing. Additionally, errors in algorithm calculations were mitigated through the application of numerical methods, both abstract and relative. Tumor area matching was achieved through the implementation of a template matching algorithm, culminating in the utilization of template matches. Furthermore, the algorithm template achieves the highest performance on hybrids when the coefficient value is +1, surpassing the optimal value of previous techniques.

4. CONCLUSION

Utilizing model methods in conjunction with pixel-based approaches has yielded optimal outcomes for both tadala and hybrid formulas by means of pixel analysis and template matching. Hence, additional advancements are required in the pixel methodology for the purpose of segmentation and extraction.

1. The suggested approach achieves a detection accuracy of 99% in distinguishing between the primary object and the tumor area in a picture. The separation of picture objects is achieved through the recognition of visual patterns using techniques such as thresholding, active contours, and Otsu's method. Additionally, a combination of active contours and Otsu's method is used, along with the creation of ground truth for each image.

2. Proposed are hybrid algorithms that combine the Otsu method with active contours for extracting tumor areas in the brain. The segmentation process in the hybrid algorithm yields pixels, which are then used in the extraction process using methods such as the Otsu method, active contour, hybrid, and template matching algorithms.
3. The accuracy calculation in this study utilizes the error methodology derived from active contour techniques, otsu , microdicom, and hybrid. The outcome can be achieved by determining the pixel size using the pixel approach, which has an average accuracy of 99%. This can be done by the numeric method, which calculates the absolute and relative errors, resulting in a value of 99%.
4. By analyzing the results of MRI imaging, researchers can conduct investigations to detect and characterize various types of brain tumors.
5. Research might concentrate on creating algorithms or other methods that can improve measurement accuracy to enhance the results of thorough measurements and the detection of brain tumor locations.

REFERENCES:

[1] V. V. Vauzia and I. D. Sumitra, "Technology of Health Services in Industrial Revolution 4.0 Era," *IOP Conf. Ser. Mater. Sci. Eng.*, vol. 879, no. 1, pp. 0–6, 2020, doi: 10.1088/1757-899X/879/1/012012.

[2] A. Finch, G. Solomou, V. Wykes, U. Pohl, C. Bardella, and C. Watts, "Advances in research of adult gliomas," *Int. J. Mol. Sci.*, vol. 22, no. 2, pp. 1–36, 2021, doi: 10.3390/ijms22020924.

[3] A. V. Faria, Z. Liang, M. I. Miller, and S. Mori, "Brain MRI pattern recognition translated to clinical scenarios," *Front. Neurosci.*, vol. 11, no. OCT, pp. 1–14, 2017, doi: 10.3389/fnins.2017.00578.

[4] P. Sasvari, "The Effects of Technology and Innovation on Society," 2013, [Online]. Available: http://arxiv.org/abs/1307.3911

[5] A. S. Parihar, "A study on brain tumor segmentation using convolution neural network," in *Proceedings of the International Conference on Inventive Computing and Informatics, ICICI 2017*, 2018. doi: 10.1109/ICICI.2017.8365336.

[6] A. Skaržauskienė, R. Tamošiūnaitė, and I. Žalėnienė, "Defining Social Technologies," *Proc. Eur. Conf. Inf. Manag. Eval.*, no. 1, pp. 239–247, 2013, [Online]. Available: http://web.ebscohost.com/ehost/pdfviewer/pdfviewer?vid=4&sid=5eaa0323-337e-4913-a9a3-ac95549e54f9%40sessionmgr112&hid=121

[7] S. Dube, S. El-Saden, T. F. Cloughesy, and U. Sinha, "Content Based Image Retrieval for MR Image Studies of Brain Tumors."

[8] I. F. Parney and M. D. Prados, "Glioblastoma multiforme," *Textb. Neuro-Oncology*, pp. 143–148, 2005, doi: 10.1016/B978-0-7216-8148-1.50022-X.

[9] C. Le Fèvre *et al.*, "Ellipsoid calculations versus manual tumor delineations for glioblastoma tumor volume evaluation," *Sci. Rep.*, vol. 12, no. 1, pp. 1–9, 2022, doi: 10.1038/s41598-022-13739-4.

[10] Z. N. K. Swati *et al.*, "Content-Based Brain Tumor Retrieval for MR Images Using Transfer Learning," *IEEE Access*, vol. 7, pp. 17809–17822, 2019, doi: 10.1109/ACCESS.2019.2892455.

[11] K. Gong, T. Shi, L. Zhao, Z. Xu, and Z. Wang, "Comparing the inter-observer reliability of the Tada formula among neurosurgeons while estimating the intracerebral haematoma volume," *Clin. Neurol. Neurosurg.*, vol. 205, no. April, p. 106668, 2021, doi: 10.1016/j.clineuro.2021.106668.

[12] D. Hasan, O. Nikoubashman, R. Pjontek, A. Stockero, H. A. Hamou, and M. Wiesmann, "MRI appearance of chronic subdural hematoma," *Front. Neurol.*, vol. 13, 2022, doi: 10.3389/fneur.2022.872664.

[13] W. M. T. Jolink *et al.*, "Contrast leakage distant from the hematoma in patients with spontaneous ICH: A 7 T MRI study," *J. Cereb. Blood Flow Metab.*, vol. 40, no. 5, pp. 1002–1011, 2020, doi: 10.1177/0271678X19852876.

[14] A. K. Maeda, L. R. Aguiar, C. Martins, G. L. Bichinho, and M. A. Gariba, "Hematoma volumes of spontaneous intracerebral hemorrhage: The ellipse (ABC/2) method yielded volumes smaller than those measured using the planimetric method," *Arq. Neuropsiquiatr.*, vol. 71, no. 8, pp. 540–544, 2013, doi: 10.1590/0004-282X20130084.

[15] J. P. Feldman, R. Goldwasser, S. Mark, J. Schwartz, and I. Orion, "Quantitative Methods Inquires 455 A MATHEMATICAL MODEL FOR TUMOR VOLUME EVALUATION USING TWO-DIMENSIONS," no. November 2008, 2014.

[16] M. Ben Abdallah, M. Blonski, S. Wantz-

Mezieres, Y. Gaudeau, L. Taillandier, and J. M. Moureaux, "Predictive models for diffuse low-grade glioma patients under chemotherapy," *Proc. Annu. Int. Conf. IEEE Eng. Med. Biol. Soc. EMBS*, vol. 2016-Octob, pp. 4357–4360, 2016, doi: 10.1109/EMBC.2016.7591692.

[17] J. Sápi, L. Kovács, D. A. Drexler, P. Kocsis, D. Gajári, and Z. Sápi, "Tumor volume estimation and quasi- continuous administration for most effective bevacizumab therapy," *PLoS One*, vol. 10, no. 11, pp. 1–20, 2015, doi: 10.1371/journal.pone.0142190.

[18] K. Mittal, A. Shekhar, P. Singh, and M. Kumar, "Brain Tumour Extraction using Otsu Based Threshold Segmentation," *Int. J. Adv. Res. Comput. Sci. Softw. Eng.*, vol. 7, no. 4, pp. 159–163, 2017, doi: 10.23956/ijarcsse/v7i4/0145.

[19] Parveen and A. Singh, "Detection of brain tumor in MRI images, using combination of fuzzy c-means and SVM," *2nd Int. Conf. Signal Process. Integr. Networks, SPIN 2015*, pp. 98–102, 2015, doi: 10.1109/SPIN.2015.7095308.

[20] A. Kumar and A. Tiwari, "A Comparative Study of Otsu Thresholding and K-means Algorithm of Image Segmentation," *Int. J. Eng. Tech. Res.*, vol. 9, no. 5, pp. 12–14, 2019, doi: 10.31873/ijetr.9.5.2019.62.

[21] H. P. Hadi, E. Faisal, and E. H. Rachmawanto, "Brain tumor segmentation using multi-level Otsu thresholding and Chan-Vese active contour model," *Telkomnika (Telecommunication Comput. Electron. Control.*, vol. 20, no. 4, pp. 825–833, 2022, doi: 10.12928/TELKOMNIKA.v20i4.21679.

[22] H. Müller, N. Michoux, D. Bandon, and A. Geissbuhler, "A review of content-based image retrieval systems in medical applications - Clinical benefits and future directions," *Int. J. Med. Inform.*, vol. 73, no. 1, pp. 1–23, 2004, doi: 10.1016/j.ijmedinf.2003.11.024.

[23] M. A. M. Shukran, M. N. Abdullah, and M. S. F. M. Yunus, "New Approach on the Techniques of Content-Based Image Retrieval (CBIR) Using Color, Texture and Shape Features," *J. Mater. Sci. Chem. Eng.*, vol. 09, no. 01, pp. 51–57, 2021, doi: 10.4236/msce.2021.91005.

[24] S. L. Bangare, G. Pradeepini, and S. T. Patil, "Brain tumor classification using mixed method approach," *2017 Int. Conf. Inf. Commun. Embed. Syst. ICICES 2017*, no. Icices, pp. 0–3, 2017, doi: 10.1109/ICICES.2017.8070748.

[25] Mehmet Kocak, "Disadvantages of MRI," University Medical Center. [Online]. Available: https://www.merckmanuals.com/home/special-subjects/common-imaging-tests/magnetic-resonance-imaging-mri

[26] G. Madhupriya, M. Guru Narayanan, S. Praveen, and B. Nivetha, "Brain tumor segmentation with deep learning technique," in *Proceedings of the International Conference on Trends in Electronics and Informatics, ICOEI 2019*, 2019. doi: 10.1109/icoei.2019.8862575.

[27] S. Sreenivasan, V. Madhugiri, G. Sasidharan, and R. V. R. Kumar, "Measuring glioma volumes: A comparison of linear measurement based formulae with the manual image segmentation technique," *J. Cancer Res. Ther.*, vol. 12, no. 1, pp. 161–168, 2016, doi: 10.4103/0973-1482.153999.

[28] P. W. Jones and M. Rabbani, "Digital Image Compression," *Digit. Image Process. Methods*, no. December, pp. 261–325, 2020, doi: 10.1201/9781003067054-8.

[29] Z. Wang, B. Li, and L. Li, "Research on water quality detection technology based on multispectral remote sensing," in *IOP Conference Series: Earth and Environmental Science*, 2019. doi: 10.1088/1755-1315/237/3/032087.

[30] G. Yang, T. Nawaz, T. R. Barrick, F. A. Howe, and G. Slabaugh, "Discrete Wavelet Transform-Based Whole-Spectral and Subspectral Analysis for Improved Brain Tumor Clustering Using Single Voxel MR Spectroscopy," *IEEE Trans. Biomed. Eng.*, vol. 62, no. 12, pp. 2860–2866, 2015, doi: 10.1109/TBME.2015.2448232.

[31] M. Vaillant and C. Davatzikos, "Finding parametric representations of the cortical sulci using an active contour model," *Med. Image Anal.*, vol. 1, no. 4, pp. 295–315, 1997, doi: 10.1016/S1361-8415(97)85003-7.

[32] R. Wongso, Meiliana, and D. Suhartono, "A literature review of question answering system using Named Entity Recognition," in *Proceedings - 2016 3rd International Conference on Information Technology, Computer, and Electrical Engineering, ICITACEE 2016*, 2017. doi: 10.1109/ICITACEE.2016.7892454.

[33] W. Gunawan, D. Suhartono, F. Purnomo, and A. Ongko, "Named-Entity Recognition for Indonesian Language using Bidirectional LSTM-CNNs," in *Procedia Computer Science*, 2018. doi: 10.1016/j.procs.2018.08.193.

[34] B. V. Isunuri and J. Kakarla, "Brain Tumor Extraction using Adaptive Threshold Selection Network," *2019 IEEE 1st Int. Conf. Energy, Syst. Inf. Process. ICESIP 2019*, pp. 1–6, 2019, doi: 10.1109/ICESIP46348.2019.8938318.

[35] C. E. Widodo, K. Adi, A. Sugiharto, B. S. Qidir Maulana, and A. Pamungkas, "Volume target delineation for brain tumor in MRI images using active contour segmentation method," *Int. J. Appl. Eng. Res.*, vol. 11, no. 16, pp. 9031–9036, 2016.

[36] P. Example, "pixels to centimeters calculator".

[37] A. R. Iskhakov, "Mathematical Methods of Modeling of Image Processing and Analysis in the Modified Descriptive Algebras of Images," *J. Comput. Eng. Math.*, vol. 3, no. 1, pp. 3–9, 2016, doi: 10.14529/jcem160101.

[38] G. V. Kumari, M. S. Prakash, P. S. Prasad, B. Srinivas, and B. Lavanya, "Image Compression using Clustering Techniques for Bio Medical Applications," *Int. J. Emerg. Technol.*, vol. 11, no. 3, pp. 1185–1193, 2020, [Online]. Available: www.researchtrend.net

[39] N. S. Hashemi and R. B. Aghdam, "Template Matching Advances and Applications in Image Analysis," 2016, [Online]. Available: http://arxiv.org/abs/1610.07231

[40] "Numerical Methods 5.1. Introduction," *N. Engl. J. Med.*, vol. 339, no. 24, pp. 1725–1733, 1998, [Online]. Available: http://www.nejm.org/doi/abs/10.1056/NEJM199812103392401